Digital Analysis of Partial Discharges

Edward Gulski

Delft University of Technology,
High Voltage Laboratory, The Netherlands

ABSTRACT

In this paper relevant aspects of digital processing of partial discharge (PD) as measured by conventional PD detection methods are discussed. Moreover, a systematic study of PD quantities is presented and discussed within the scope of practical PD analyzes, including recognition of defects in certain HV insulation configurations.

1. INTRODUCTION

THROUGH the years, many methods for detection, location and evaluation of PD phenomena have been developed [1–19]. Moreover, many discharge quantities were introduced in order to improve this situation [4, 12]. Although the quantities used today do not predict the lifetime of dielectric insulation in particular HV equipment, they do give information on its quality. PD measurements often provide a means for detecting defects that otherwise would lead to the breakdown of the dielectric. In general, there are six types of PD, see Figure 1, [7, 9]:

1. Corona discharges occur at sharp points protruding from electrodes in gases and in liquids.
2. Surface discharges may occur in gases or in oil if there is a strong stress component parallel to the dielectric surface.
3. Internal discharges occur in gas-filled cavities, but oil-filled cavities can also break down and cause gaseous discharges afterwards.
4. Electric trees can start from sharp conducting particles or from a cavity in solid insulation.
5. Floating part discharges occur in cases of badly grounded components in or near a HV circuit.
6. Contact noise may occur in cases of bad contacts or poor grounding of the test samples.

In practice the most used PD measurement is electric pulse detection [1, 3, 6, 13–16]. This method is based on the measurement of the current impulses caused by a discharge in the defect and which occur in the circuit in series with the dielectric. The following three goals are important here: to determine the presence of PD and to estimate their magnitude; to locate the site of the discharges; and to estimate the danger caused by the detected discharges. Therefore, information on the type of defect is important [9, 20, 21].

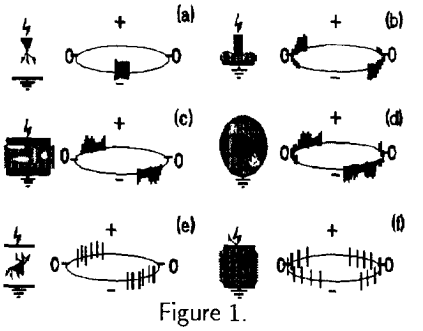

Figure 1.

Typical insulation defects and their stylized discharge patterns. (a) corona discharges, (b) surface discharges, (c) cavity discharges, (d) treeing discharges, (e) floating part, (f) contact noise.

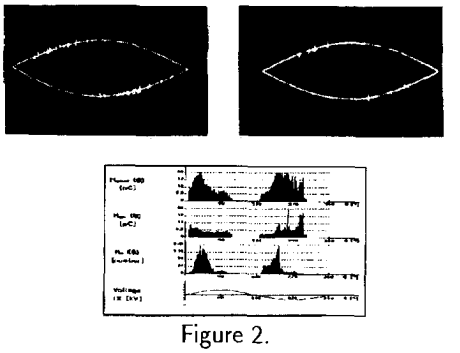

Figure 2.

PD patterns as observed during PD measurement on a 3 nF, 100 kV capacitor. (a) photograph of cathode ray screen as made within 2 min, (b) phase-resolved distributions as processed during 2 min.

It is known that the characteristics of discharges may

change substantially during service and that the occurrence of discharges depends among other things on temperature, pressure, applied voltage and the test duration. The occurrence of discharges may cause structural changes in the defects so that the discharge patterns may be subject to change [4, 10, 11]. To analyze the PD process, oscillograms give valuable information about the type and origin of discharges; moreover diagrams of discharge magnitude as a function of voltage also help to determine the cause of discharges [3–9, 12]. The changes in the behavior of discharge magnitude and extinction voltage may add to these findings. However, the combination of these characteristics gives an indication only, and much depends on its intelligent use. Room is left for considerable doubt. An example of patterns that undergo change over a short time is shown in Figure 2(a). It follows from Figure 2(b) that the PD process as observed during 2 min also can be described using digital quantities representing typical patterns for this period.

In recent years, investigation into the use of digital techniques for the evaluation of PD has become increasingly important. The trend towards automation in tests for cables, transformers and other insulated devices is evident [8, 11, 18–22]. One of the undoubted advantages of a computer-aided measuring system is the ability to process a large amount of information and to transform this information into an understandable output.

Many computer aided systems have been developed for the measurement and understanding (evaluation and interpretation) of PD phenomena [12, 13, 17–26, 28–31]. In this way a complete data recording can be made and a basis will be created for further evaluation and diagnosis of the insulating systems. This trend concentrates on the development of the recognition of discharge sources and the evaluation of measuring results [23–52].

Nevertheless, the PD process in a defect is sensitive to many factors such as roughness of the interface surface, aging process, local field strength, *etc.* All these parameters may influence the measured PD pulse sequence which is the basis for in-depth analysis. Moreover these parameters may influence the outcome of the digital system [56]. Therefore, human experience is essential for the evaluation of results, even if obtained by a digital system.

In this paper important aspects as related to digital processing of PD measuring data will be discussed: digital acquisition of PD sequences, signal processing and analysis possibilities, and diagnosis of defects in HV insulation.

2. DIGITAL ACQUISITION OF PD SEQUENCES

Since the last revision of the IEC 270 Standard for PD measurements (1981) much effort has been put into electrical measurement of PD, but above all in the development of new, often computer-aided measuring systems. Since 1993 the above mentioned IEC Standard has been under revision, where recommendations regarding digital PD measurement will comprise part of the new Standard. Therefore, in this Section some fundamental aspects of the digital processing of PD pulses will be discussed.

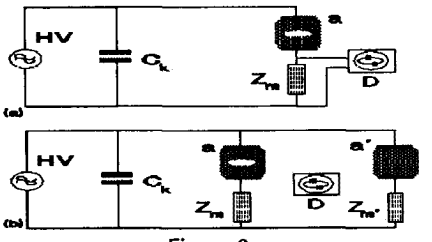

Figure 3.

Detection circuits for PD. (a) straight detection, (b) balanced detection.

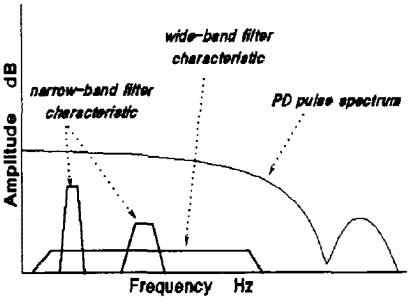

Figure 4.

Typical bandpass filter characteristics of PD measuring systems.

Basically, all modern systems measure discharges using the same PD detector as introduced in 1941 by Austen and Whitehead [1]. In Figure 3(a) this basic circuit is shown and in Figure 3(b) the balanced PD detector as later introduced by Kreuger in 1961 [3]. This circuit is principally composed of a coupling capacitor to stabilize the voltage across the test object and to pass the fast charge transfer to the test object, a measuring impedance to quantify the charge transfer by an integration of the current pulses and an instrument (PD detector) to measure or to display the PD pulses. Depending on the electrical parameters of the test circuit and of the discharge process, different characteristics can be obtained. To provide a correct integration of a discharge pulse, the upper limit f_2 of the frequency range of an analog instrument shall be $< 1/3$ of the resonance frequency of

the test object [6]. For this reason, most analog instruments have a bandwidth with upper limit < 500 kHz and $\Delta f \leqslant 400$ kHz. smaller than ~ 300 kHz. As a result, narrow-band and wide-band measuring systems have been used, see Figure 4.

Due to the increasing automatization of PD measurements in recent years the use of digital systems has become very popular. A computer-aided system containing a digital memory offers the opportunity to store the discharge pulse sequences and to postprocess these in the course of time or as a function of the power frequency cycle. For this purpose several deduced quantities exist and they have a practical implication [4, 6, 7, 26]. Most of these quantities are related to the magnitude and the phase-position of a PD pulse. Consequently, the value of all these parameters strongly depends on the correct digital registration of the discharge sequences.

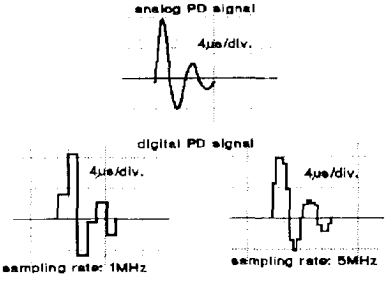

Figure 5.

Digitized PD pulses as measured by PD system with a bandwidth of 40 to 400 kHz using different sampling rates.

2.1. DIGITAL PD DETECTOR

Generally, a digital instrument samples and stores the individual PD pulses after continuous quasi-integration of the discharge-current pulses using an analog instrument. It means, that in addition to an analog instrument, a digital instrument shall continuously register the peak values of individual pulses. Due to the fact that the pulse shape of a discharge is determined by the resonance frequency of the discharge circuit, the digitization of discharge pulses should not concentrate on the shape of the PD pulse, but on the registration of the peak values of the discharge pulses, see Figure 5.

Moreover, with regard to maximum time of registration and data processing for which the digital instrument is designed, distinction may be made between two types of digital instruments, a detector and an analyzer.

A system for short test times is a digital PD detector. The instrument displays and stores the peak value of the apparent charge. For this purpose the discharge sequence has to be measured and displayed during ~ 500 s.

A system for long test times is a digital PD analyzer. The instrument measures and displays not only the apparent charge but also processes several derived quantities for an in-depth analysis. During the test the discharge sequences are processed and stored from ~ 100 s to ~ 100 h. In this case, due to the large amount of information, compression procedures can be applied; for instance averaging, peak storage or signal integration.

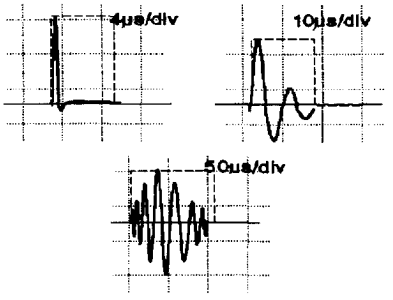

Figure 6.

Output voltage signals of three different PD measuring systems for apparent charge.

2.2. SPECIFIC REQUIREMENTS

The important difference between analog and digital instruments is that digital signals contain no information between individual samples of the measured signal. In consequence, the peak value of the discharge pulse can be approximated only. To obtain the peak value of discharge pulses two measures are recommended. First, after the quasi-integration of the discharge current pulses, using sufficiently high sampling rates $f_s > 10 f_2$, the discharge pulses are digitized and stored as numerical values. To determine the peak value of the discharge pulse these numerical values must be interpolated using mathematical routines to produce a curve similar to the curve recorded by an analog instrument, see Figure 6.

Second, after the quasi-integration of the discharge current pulses and before digitization, an analog circuit must be used to capture the peak value of the discharge pulse. Using a sample and hold circuit a rectangular pulse can be generated with an amplitude proportional to the peak value of the discharge pulse. In this way the resolution time of the digital instrument may be adjusted to the pulse resolution of the analog instrument only [50].

To give an example, it is known that in the case of corona discharges at ac voltage the discharges are symmetrically disposed about the voltage peak, and are of equal magnitude and equally spaced in time. In Figures 7 to 9 examples of corona discharges at HV point are analyzed using different diagrams of discharge magnitude and discharge intensity. The main objective of these examples is to show the importance of correct digitization. In all

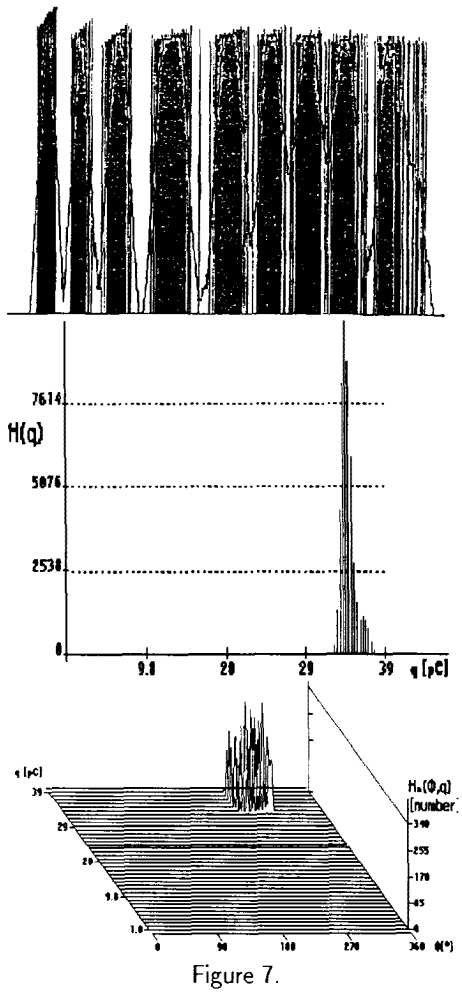

Figure 7.

Measured data of corona discharges processed for 2 min at 4 kV. Sample: single point-to-plane configuration at the HV electrode in air; point diameter 50 μm, distance to plane 50 mm; Bandwidth: 40 to 400 kHz, Time resolution: 6 μs.

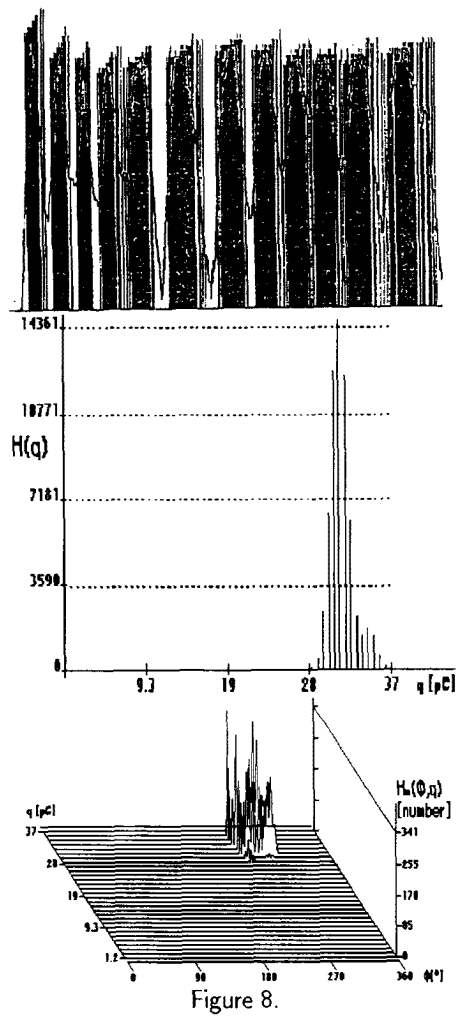

Figure 8.

Measured data of corona discharges processed for 2 min at 4 kV. Sample: single point-to-plane configuration at the HV electrode in air; point diameter 50 μm, distance to plane 50 mm; Bandwidth: 70 to 80 kHz, Time resolution: 150 μ s.

cases during 2 min the same well defined point-plane configuration at HV electrode was studied. It is known that this configuration is characterized by stable behavior in PD magnitude and PD intensity. To test the influence of resolution time of the instrument on different PD pulses as detected by different band-pass filter characteristics two bandpass filters were used: wide band of 40 to 400 kHz and narrow band of 70 to 80 kHz. It can be seen from Figures 7 and 8 that selecting the correct resolution time of the digital instrument for a certain filter characteristic of the PD detector provided correct measurement of the PD magnitudes. On the other hand, Figure 9 shows that a wrong time resolution of the digital instrument may falsify the measurement result of discharge magnitude.

It follows, from this example, that complete in-depth analysis as is usual by computer-aided processing may be strongly influenced or even falsified by incorrect digitization of PD pulses.

When using a digital PD detector, another important aspect needs special attention: the reading of the digital PD meter. It is evident that independent of the kind of PD detector, analog or digital, the value of recorded PD magnitude has to be the same. Finally, most actual standards or specifications of different apparatus are based on analog PD detection.

It is known that in the case of an analog PD peak meter (with certain charging and discharging time constants) the reading in pC is based on the largest repeatedly occurring magnitude. In other words, the final value in pC as displayed by the instrument is based not on a single PD discharge event, but is a result of a certain relationship between the measured PD magnitudes and their pulse repetition rate, for more information see for

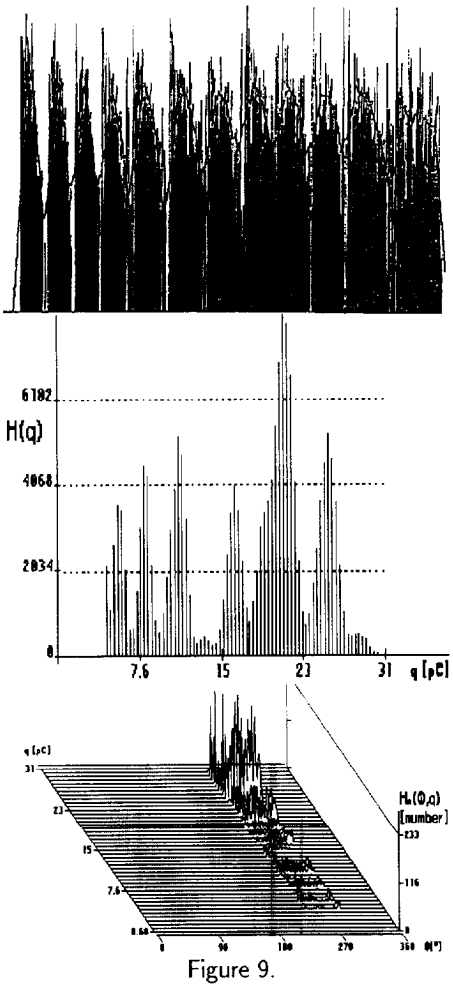

Figure 9.

Measured data of corona discharges processed for 2 min at 4 kV. Sample: single point-to-plane configuration at the HV electrode in air; point diameter 50 μm, distance to plane 50 mm; Bandwidth: 70 to 80 kHz, Time resolution: 6 μs.

instance the normalized evaluating function as described in (IEC) CISPRE 16–1.

After digital processing of a PD sequence a digital PD instrument is able to display two values: the magnitude of the single PD event as observed during the test, and also statistically processed values. For this purpose, based on an intensity distribution of PD pulses, the most appropriate statistical parameters have to be selected *e.g.* mean value of specific percentile quartiles of this distribution or simply the mean value of all maximum PD pulses as observed during 1 s in each power frequency cycle. In this way a digital indication will be available having similar characteristics as the analog PD reading.

Therefore the following characteristics require more attention during testing and calibration of a digital PD system and, preferably be specified in a kind of performance rapport of the digital PD detector/analyzer: the time resolution of two consecutive discharge pulses, in μs or in °; the discharge singularity or identity of one discharge pulse is independent of the frequency characteristic of the measuring circuit, one peak value from the calibrator is represented by one digital value; the continuity of the digital acquisition for which a check is necessary to ensure that within the specified repetition rate of the particular digital instrument no single discharge impulse is lost during the registration; and the procedure for specifying the PD reading in pC.

3. PD QUANTITIES FOR EVALUATION OF HV MEASUREMENTS

In practice the evaluation of PD in HV constructions is restricted to measuring the inception voltage (in kV) and largest discharge magnitude (in pC) and comparing these to the test specifications. However, if the maximum allowable discharge level is exceeded, it is important to know the cause of the discharge. For this purpose different discharge related quantities have been introduced in the past and are still in use. Also, the use of a computer-aided system offers the opportunity to store sequences of the discharge pulses and to postprocess these in the course of time or as a function of the power frequency cycle. In this way a basis is created for further evaluation and diagnosis of the insulating systems.

The main goal of this Section is to make an inventory of some analysis and presentation methods which may have a practical implication for the evaluation of PD measurements.

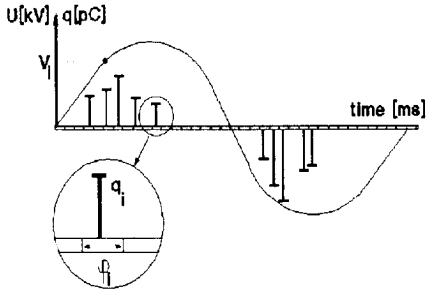

Figure 10.

The basic discharge quantities q_i, ϕ_i and V_i which describe the PD activity in the case of conventional PD detection.

3.1. PD DERIVED QUANTITIES

A digital PD analyzer which provides registration of the discharge signals and the test voltage may process the discharge magnitude and the discharge position related to the power frequency cycle. Using a classic PD detector the following quantities are the basic ones to describe the recurrence of discharges, see Figure 10. The discharge

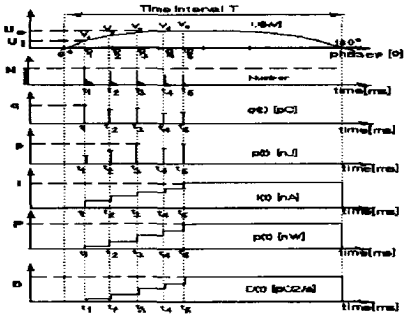

Figure 11. Diagram of PD quantities.

magnitude q_i represents the peak value in pC of the single discharge pulse. The discharge phase ϕ_i represents in the phase position of q_i as related to the power frequency cycle. The discharge instantaneous inception voltage V_i represents the momentary value in kV of the test voltage at which the discharge q_i has occurred.

All other quantities which were introduced throughout the years, and which may have practical implications for the analysis of discharges are calculated on the basis of these three. If the PD measurements are performed during a time interval T several quantities can be processed by a digital instrument, see Figure 11. The duration of T is either the positive half or the negative half of the power frequency cycle, or possibly the duration of the whole cycle of the power frequency. Also, in the case of a wide-band PD instrument, the positive or negative half of the power frequency cycle can also be replaced by the polarity of discharge pulses. For both cases the following PD quantities are frequently in use: q, p,U_i U_e, I, P, N, and D.

The discharge magnitude q is the maximum value of discharge magnitude q_i observed during the time interval T. The discharge energy p is the maximum value of the discharge energy magnitude $p_i = q_i V_i$ observed during the time interval T. Due to the fact the derivation of this quantity is phase angle dependent it may in certain cases result in negative contribution by particular pulses [59].

The discharge phase inception voltage U_i is the momentary voltage during each half cycle where the discharge pulse sequence starts, while the discharge phase extinction voltage U_e is the momentary voltage during each half cycle at which the discharge pulse sequence stops. The discharge current is $I = 1/T \times \sum |q_i|$, where T is the duration of the power frequency half cycle is and the i the number of the consecutive discharge as observed during T, the discharge power $P = 1/T \times \sum |q_i U_i|$, the discharge intensity N is the total number of discharges as observed during T, and the quadratic rate $D = 1/T \times \sum q_i^2$.

If the observation time t takes place for longer than T, *e.g.* > 100 power frequency cycles, the above mentioned quantities may be further processed by calculating during t the maximum, average, or integrated values. Moreover, all these quantities can either be analyzed as a function of time but also as a function of the phase angle. Consequently, three groups of quantities can be distinguished as shown below.

3.2. ANALYSIS AND DISPLAY METHODS

3.2.1. TIME FUNCTIONS OF DERIVED QUANTITIES

The first group consists of quantities processed either during the positive half or the negative half of the voltage cycle as follows: the discharge magnitude $q(t)$, the momentary inception phase voltage $U_{inc}(t)$, the momentary extinction phase voltage $U_{ext}(t)$, the discharge current $I(t)$, the discharge energy magnitude $p(t)$, the discharge power magnitude $P_i(t)$, the number of discharges $N_q(t)$, and the quadratic rate $D(t)$.

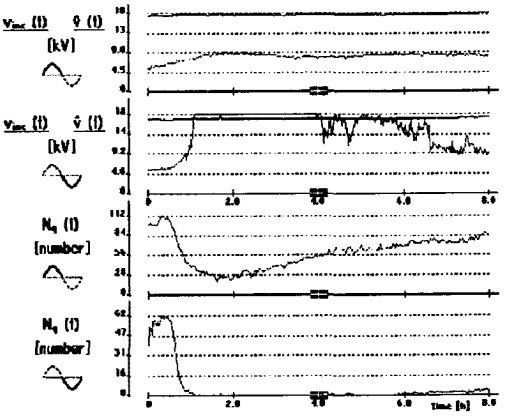

Figure 12.

PD quantities the phase inception voltage $U_{inc}(t)$ and the number of discharges $N_q(t)$ as observed during 8 h for surface discharges.

It is known that the behavior of discharges may be very complex due to their dependency to a wide range of conditions at the discharge site, and to the voltage level. Moreover, depending on 'aging effects' at the discharge site, different types of behavior can be observed in the course of time [43]. In Figures 12 and 13 two examples are given. They show two PD quantities of surface discharges as observed during 8 h and the same PD quantities of internal discharges in a flat cavity as observed during 65 h. Looking at these diagrams the characteristic behavior of the number of discharges $N_q(t)$ can be observed: a clear decrease in the case of flat cavity, and an increase in the positive half of the voltage cycle by surface discharges. Further, differences in the inception voltage $U_{inc}(t)$ can also be observed: an increase for the flat cavity and a decrease after 4 h in the case of surface

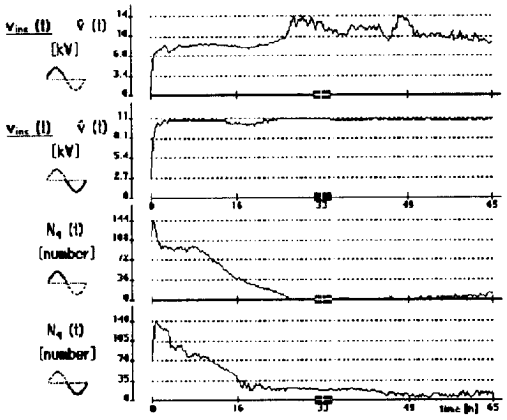

Figure 13.

PD quantities the phase inception voltage $U_{inc}(t)$ and the number of discharges $N_q(t)$ as observed during 65 h for cavity discharges.

discharges. In both cases the changes in behavior can be explained in terms of aging effects at the discharge site [54, 58].

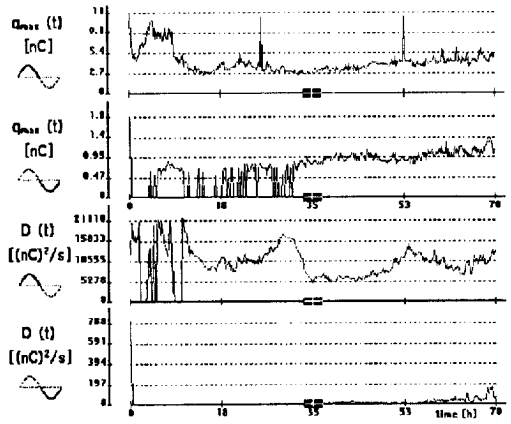

Figure 14.

PD quantities maximum discharge magnitude $q_{max}(t)$ and the quadratic rate $D(t)$ as observed during 70 h for surface discharges.

In Figure 14 examples of changes in discharge magnitude $q_{max}(t)$ and quadratic rate $D(t)$ are shown. Both quantities were observed for surface discharges during 70 s. It can be seen from this Figure that in contrast to $q_{max}(t)$ the quantity $D(t)$ is characterized by more changes in the positive half of the voltage cycle [60]. Similar to the results as shown in Figures 12 and 13 the explanation of these changes can be found in the physical changes of the dielectric surface.

3.3. INTENSITY HISTOGRAMS OF DISCHARGE AND ENERGY MAGNITUDES

The second group of quantities comprises the intensity histograms. In this way the number of pulses as a function of apparent charge or discharge energy magnitude can be described as $H(q)$, the distribution of the discharge magnitude, and $H(p)$ the distribution of the discharge energy magnitude.

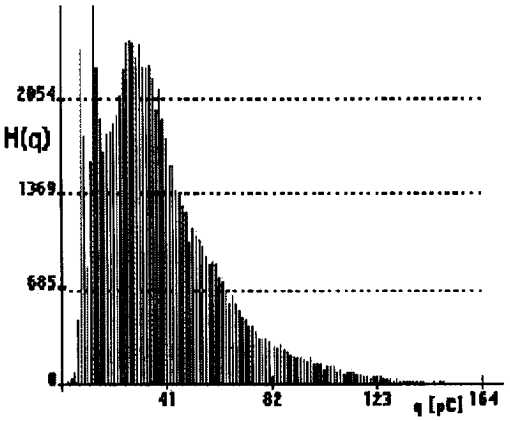

Figure 15.

The intensity spectrum of discharge magnitude as observed for five cavities electrode-bounded in polyethylene.

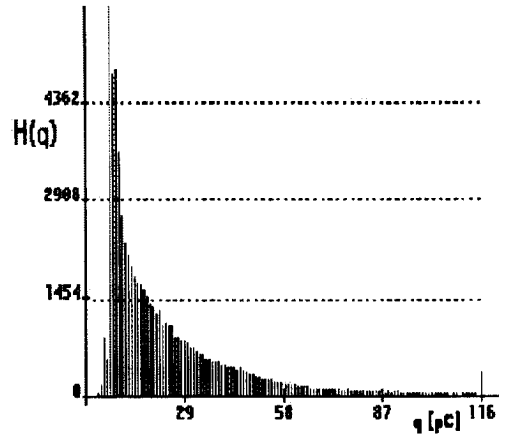

Figure 16.

The intensity spectrum of discharge magnitude as observed for a single flat cavity in polyethylene.

The observation of these intensity spectra can give interesting additional information about discharge sources. In Figures 15 to 17 three spectra are shown of discharge magnitudes observed for multiple cavities discharges, single point corona at the HV electrode and discharges between two touching insulators. The differences are clearly visible and it is clear that using this PD quantity additional information can be obtained to analyze different PD sources [50].

3.4. DISTRIBUTIONS OF PHASE-RELATED DERIVED QUANTITIES

The discharge quantities as function of the phase angle belong to the third group. The discharge magnitude is

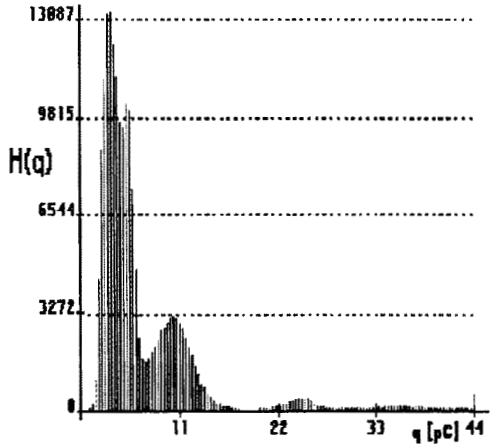

Figure 17.

The intensity spectrum of discharge magnitude as observed for surface discharges between two touching insulators.

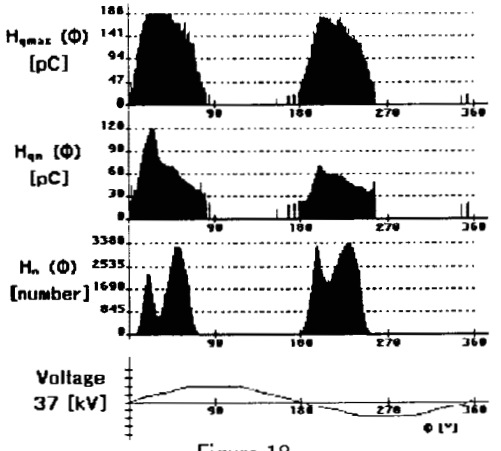

Figure 18.

The phase-resolved quantities as observed for discharges in a flat cavity.

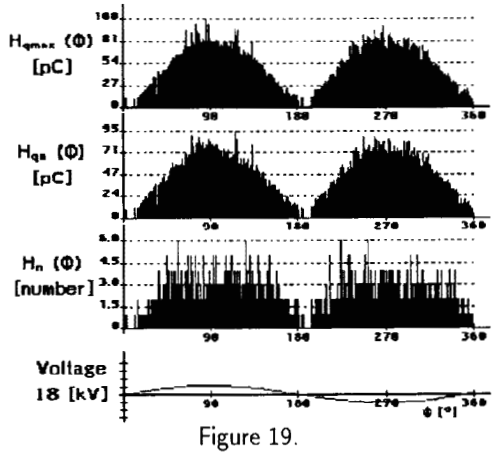

Figure 19.

The phase-resolved quantities as observed for discharges in air bubbles in oil.

analyzed as a function of the power frequency cycle. For this purpose the power frequency cycle is divided in several phase windows ϕ_i representing the phase angle axis ($0 \ldots 360^\circ$), see Figure 10. As a result, during the digitization and the storage of discharge pulses their position as related to the power frequency may be measured. For comparison, the width of one phase window ϕ_i should be equal to the time resolution of the digital instrument.

If the observation takes place during time t, the integral distribution of individual discharge events may be observed in each phase window ϕ_i. Moreover, these distributions may be analyzed using the sum of the discharge magnitudes in each phase window ϕ_i, the number of discharges in each phase window ϕ_i, and the maximum value of the discharge magnitude in each phase window ϕ_i.

These quantities, when observed throughout the whole cycle ($0 \ldots 360^\circ$) result in the following four distributions. $H_{\Sigma q}(\phi)$ is the distribution of the sum of discharges, $H_n(\phi)$ the distribution of the number of discharges, $H_{qmax}(\phi)$ the distribution of the maximum values of discharges, and $H_{\Sigma q}(\phi)/H_n(\phi) = H_{qn}(\phi)$ is the distribution of the average values of discharges.

In Figure 18 an example of phase distributions is shown as observed in a flat cavity. Looking at these distributions it's clear that each distribution is characterized by its specific shape. These shapes can be explained in terms of PD inception conditions, thus reflecting the physical conditions in the cavity. The $H_{qmax}(\phi)$ sinusoidal shape of the maximum charge in a flat cavity can be related to the overvoltage in the cavity (actual field/minimum breakdown field). The flat shape of $H_{qn}(\phi)$ can be related to the type of the cavity (flat, square or narrow). The multiple peaks in the number of discharges $H_n(\phi)$ reflect the statistical occurrence of the discharges. In Figures 19 and 20 examples of other PD sources are shown. In both cases the discharge mechanism typical for these defects is clearly visible in the shapes of $H_{qmax}(\phi)$, $H_{qn}(\phi)$ distributions. In Figure 19 the sinusoidal shape of these distributions indicate multiple PD in spherical cavities. In an other example, see Figure 20, the symmetric occurrence of PD pulses about the voltage peak and their equal spacing in the time confirms corona discharges. All the above discussed PD quantities can also be analyzed as a function of time, see Figures 21 and 22. For this purpose the total observation time t is then divided into several test intervals. In each interval these distributions may be processed as a function of the power frequency cycle. In this way a PD measurement can reflect significant changes during a long-term test or during an increasing voltage test.

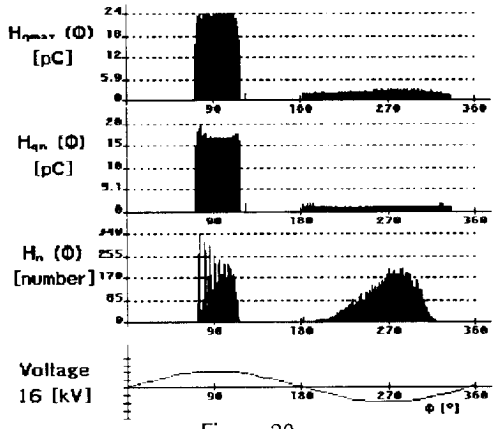

Figure 20.

The phase-resolved quantities as processed for corona discharges using sharp points at the HV electrode.

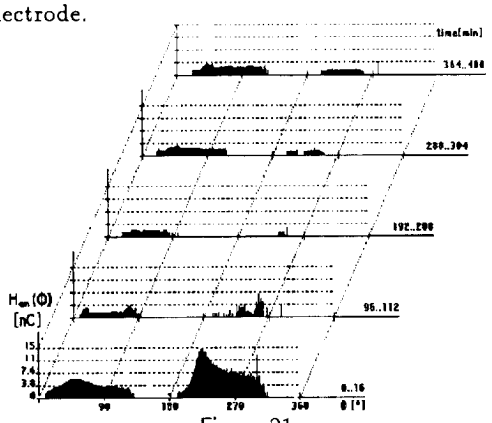

Figure 21.

Different shapes of phase-resolved quantity $H_{qn}(\phi)$ as observed during 8 h for surface discharges.

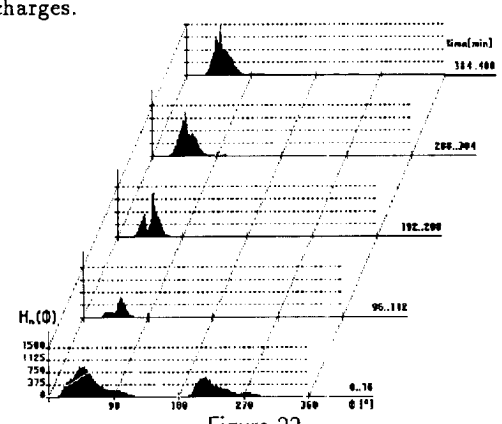

Figure 22.

Different shapes of phase-resolved quantity $H_n(\phi)$ as observed during 8 h for surface discharges.

3.5. SPECIAL GRAPHICS OF DERIVED QUANTITIES

Additionally to the PD quantities as described above the following two analysis and presentation methods are frequently used to evaluate PD.

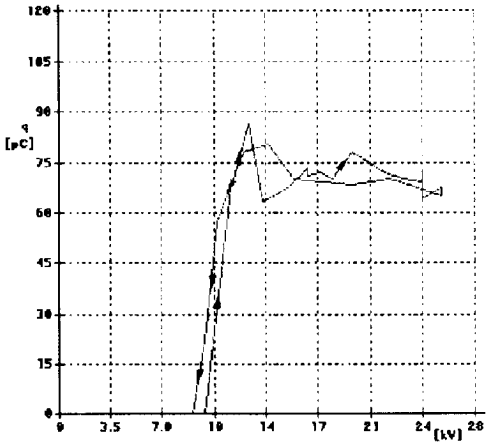

Figure 23.

The qU curve as observed for internal discharges in a 23 kV epoxy insulator.

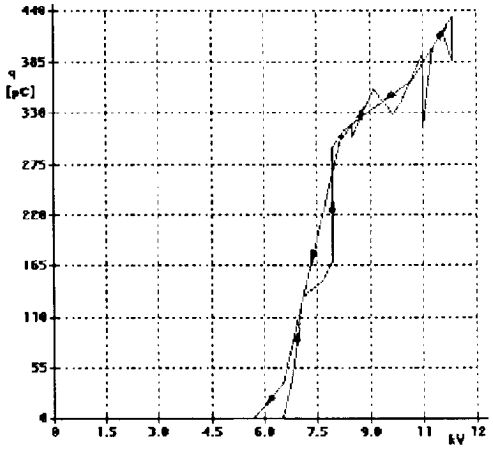

Figure 24.

The qU curve as observed for internal discharges in a 23 kV epoxy insulator.

3.5.1. THE qU CURVE

To analyze the effects of different test voltages on the discharge magnitude these may be displayed using two dimensional diagrams, where the x-axis represents the level of the test voltage in kV and the y-axis represents the level of discharges in pC. Two examples of this qU curve (which was introduced by CIGRE in 1961) are shown in Figures 23 and 24. In both cases internal discharges in the same type of epoxy resin insulator were measured.

It can be seen from these diagrams that internal discharges within the same type of HV construction may be characterized by different behavior. The qU curve in Figure 23 shows little variation in discharge magnitude when the voltage is raised above the discharge inception level. This behavior is similar to that described in a CIGRE

workgroup report on internal discharges in a dielectric-bounded cavity. On the other hand, in Figure 24, the discharge magnitude steadily increases as the voltage is raised above inception, which is more characteristic for internal discharges between conductor and dielectric in a number of cavities of various sizes. In both cases the discharge sources were for different air gaps inside the epoxy resin insulator [55], see Figure 39.

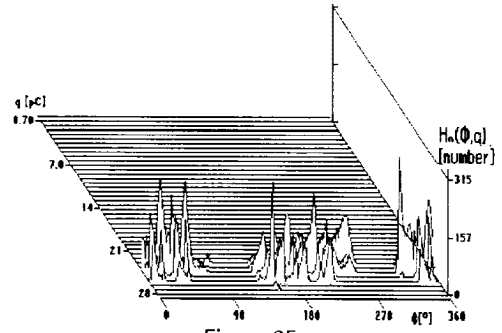

Figure 25.

The $H_n(\phi, q)$ distribution as observed for contact noise.

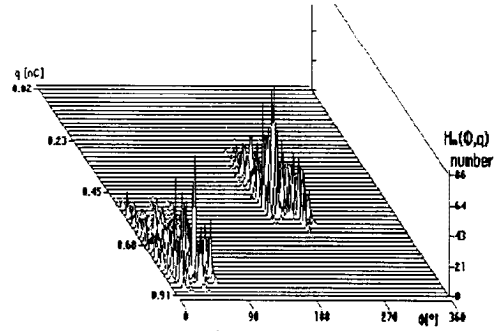

Figure 26.

The $H_n(\phi, q)$ distribution as observed for floating part discharges.

3.5.2. THE $H_N(\phi, q)$ DISTRIBUTION

To display a 3-dimensional relationship between discharge magnitude, discharge intensity and phase angle the $H_n(\phi, q)$ distribution is used. In Figures 25 and 26 examples of this presentation are shown. It is known that the 3-dimensional diagram can be very useful in analyzing the discharge process in actual HV equipment.

4. DIAGNOSIS OF DEFECTS IN HV INSULATION

The main goal of the PD diagnosis is to recognize the insulation defect which causes the discharges *e.g.* internal or surface discharges, corona, treeing, *etc.* This information is vital for estimating the harmfulness of the discharge. As shown in previous Section, using classical detection the patterns of phase-resolved data can be studied which occur in the 50 or 60 Hz sinewave. These patterns are familiar to us in the shape of the widely used ellipse on the line frequency time base. Based on the fact that each discharge pulse reflects the physical process at the discharge site, in the past a strong relationship has been found between the shape of these patterns and the type of defect causing them. As a result phase-resolved recognition using a digital system offers a number of advantages, especially for use on some industrial components [52].

First, there is no difference between the actual electrical path and that seen by the PD detector [6]. Second, the type of detector or its coupling circuit do not influence the result, because the shape of the single pulse is not relevant, only their relative height and phase angle [6]. Moreover, standard detectors of a HV laboratory can be used, because the equipment for recognition is added to the detector and is not replacing it.

In general, a system for recognition of discharges can be used in different ways. It means that the ability of digital PD analyzers to process and to store the specific information of discharge can be used for different purposes much as discharge recognition, and condition monitoring. To illustrate these possibilities, three different cases of PD recognition in HV components are discussed. For this purpose a concrete, recently commercialized fingerprint technique TEAS will be used [43, 50, 54–56]. Of course, general conclusions can be drawn, based on this particular solution with regard to digital processing.

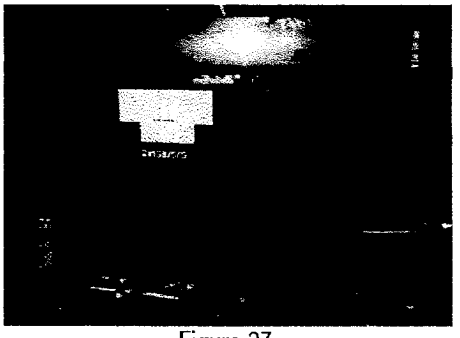

Figure 27.

Photograph of the 2×150 A to 5 A epoxy insulated current transformer.

4.1. RECOGNITION OF DISCHARGES USING ARTIFICIAL DEFECTS

It is known that simple models of discharges can be used to study complete HV constructions [43, 56]. In a particular case, a collection of 17 different discharges [43, 56] as made using simple two-electrode models is used for analysis of discharges in a 50 kV epoxy resin current transformer, see Figure 27. The origin of discharges in this type of transformer was related to several cracks around the transformer core which remained after

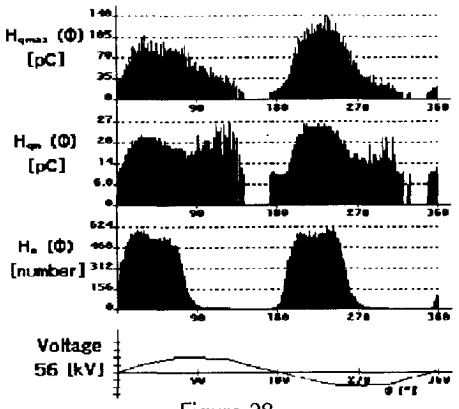

Figure 28.

The phase-resolved quantities as observed during 2 min test for discharges in the transformer.

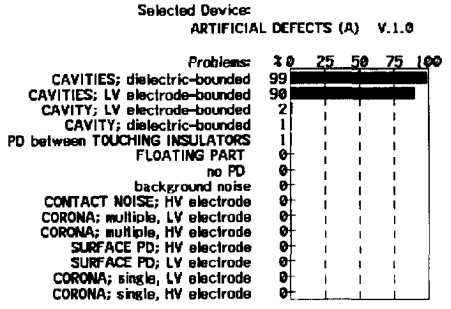

Figure 29.

Recognition by a computer-aided data bank 'artificial defects' of discharges as observed for 2 min on epoxy resin 50 kV; the origin of discharges was air cracks around the transformer core.

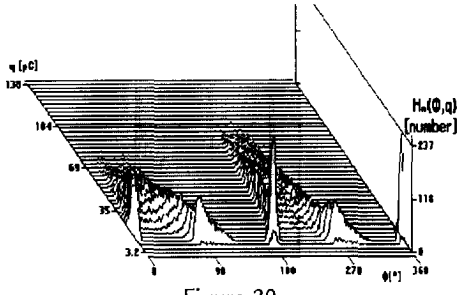

Figure 30.

The $H_n(\phi, q)$ distribution as observed during 2 min test for discharges in the transformer.

a short-circuit test. This transformer was tested during 2 min at 56 kV test voltage. In Figures 28 and 29 the phase-resolved quantities as well as the result of the comparison to 'artificial defects' are shown. In Figure 30 the 3-dimensional distributions $H_n(\phi, q)$ as observed for above mentioned discharges are shown. It follows from the classification diagram that the discharge in the transformer is caused by cavities, with a probability of 99% for dielectric or 90% for electrode bounded cavities. This result is reasonable, since there were pockets of air detected around the coil. This example shows the possibility of digital PD analyzer to recognize industrial defects using physical models of discharges.

4.2. RECOGNITION OF DISCHARGES USING INDUSTRIAL PROBLEMS

The experiences have shown also that the recognition of industrial defects depends on how near the artificial defects come to actual cases. Moreover, factors such as roughness of the interface surface, the shape of the defect, the aging process, or local field strength of a particular defect in real component may influence the measured PD sequence which is the basis for the recognition. With regard to a particular HV system, a number of discharges can occur, which are only specific for this component, and making a general model does not make much sense.

Therefore it is equally important to develop a second type of data bank which contains specific problems of a particular HV component, such as the specific location of one or several discharges in the sample. As a result, the measurements of these discharges can form a collection of specific problems. Such a collection is of importance, when in the future similar situations may occur.

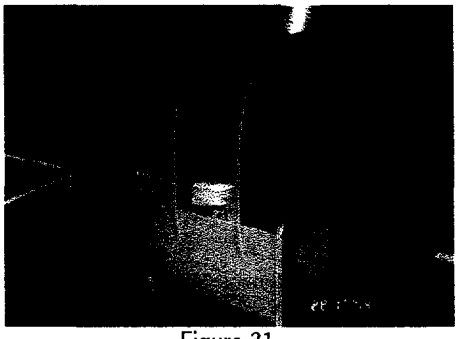

Figure 31.
Photograph of the 23 kV epoxy insulated bushing.

The following practical example is presented, called 'PD location in 23 kV bushing', see Figure 31. In particular this three-phase epoxy insulated 23 kV bushing was rejected because of measured internal discharges at 23 kV in all three phases, 230 pC in phase A, 170 pC in phase B, and 220 pC in phase C.

The main goal of further investigation was to locate, in this three-phase system, the possible discharge sites. It is known, that in the case of three-phase constructions, and single-phase energizing there are seven possible combinations (A, B, C, A+B, B+C, A+C, A+B+C) that can be used for straight PD detection.

Using these combinations, and by varying the test voltage between $0.6U_o$ and $2.2U_o$ a series of tests was made using a digital PD analyzer. To analyze the measuring data and to recognize possible discharge sites cluster

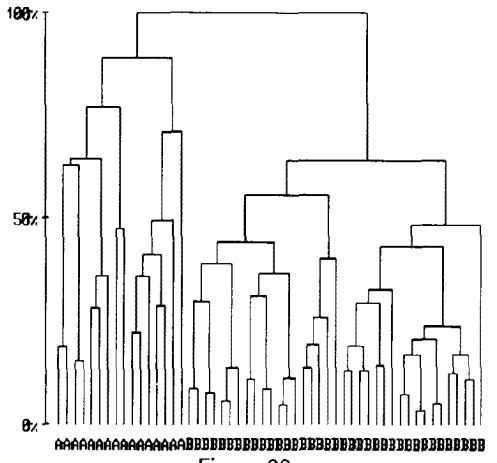

Figure 32.

Tree structure processed using the group averaging method for measuring data of a 23 kV bushing as collected at different phases and voltages.

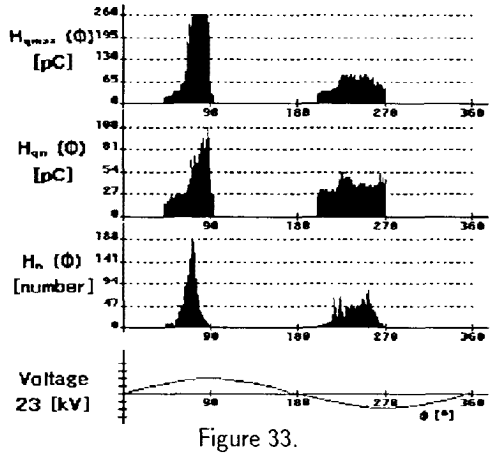

Figure 33.

The phase-resolved quantities as observed during 2 min test on phase A for 23 kV epoxy resin insulated bushing.

analysis techniques was used. By means of these tools a clustering of data without *a priori* knowledge can be recognized. In particular, using group averaging method all measuring data were sorted in the form of a tree [58]. By means of such a tree structure the similarity between different measurements can be investigated, see Figure 32. The percentage scale in this Figure shows the dissimilarity between particular measurements. It follows that similar measurements are connected at relatively low dissimilarity level, and different data are connected at higher levels. It follow from this Figure that two main groups are observed on the base of all measured data: group A and group B. Further analysis of this tree structure indicated that the left group A represents discharges between phase A and B and the right group B represents discharges between phase B and C. In Figures 33 and 34 the phase-resolved distributions are

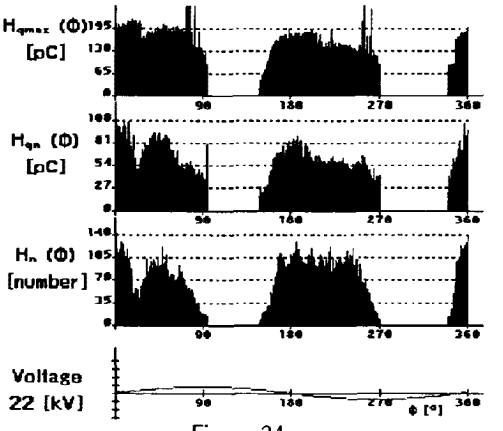

Figure 34.

The phase-resolved quantities as observed during 2 min test on phase C for 23 kV epoxy resin insulated bushing.

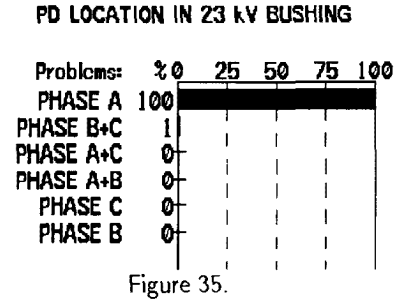

Figure 35.

Recognition by computer-aided data bank 'PD location in 23 kV bushing' of discharges as observed during 2 min test on phase A for 23 kV epoxy resin insulated bushing.

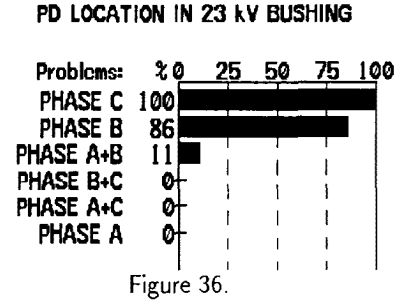

Figure 36.

Recognition by computer-aided data bank 'PD location in 23 kV bushing' of discharges as observed during 2 min test on phase C for 23 kV epoxy resin insulated bushing.

shown as observed for these two different discharge sites and in Figures 35 and 36 the results of the recognition. In particular, a data bank was developed representing the collection of internal discharges at different phases.

In Figures 37 and 38 the 3-dimensional distributions

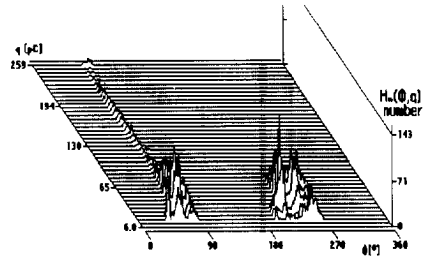

Figure 37.

The $H_n(\phi, q)$ distribution as observed during 2 min test for discharging defect between phase A and B of the 23 kV bushing.

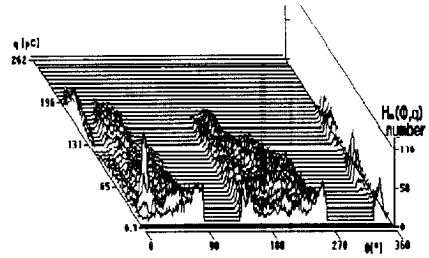

Figure 38.

The $H_n(\phi, q)$ distribution as observed during 2 min test for a defect between phase B and C of the 23 kV bushing.

$H_n(\phi, q)$ as observed for the above mentioned discharges are shown. As shown also in Figure 30, different insulation defects are characterized by typical differences in the landscape of such 3-dimensional figures. It confirms the opinion that these $H_n(\phi, q)$ distributions as mentioned here might be very useful to analyze the discharge processes in actual HV equipment [39, 45, 56].

This example shows the possibility of a digital PD analyzer to develop a user specific data bank that contains specific industrial problems.

4.3. MAPPING OF DISCHARGES USING PERIODIC MEASUREMENTS

One of the important tasks which can be done by a digital PD analyzer could be the mapping of degradation changes of discharging dielectrics. It is well known from the past and has recently been shown in detail, that with conventional detection equipment, the temporal change in discharge patterns can be observed [55, 57, 58]. Finally using similar techniques the condition of the insulation could be tested in such way. To illustrate such mapping techniques, long term aging until breakdown will be discussed here [55].

A 23 kV epoxy insulator containing air pockets around the ceramic core, see Figure 39, was aged during a period of 1606 h. To achieve a significant aging of the sample, the voltage was increased in 5 kV steps from 28 to 82 kV, every $\sim$ 150 h. During the whole aging period 45 PD measurements at 23 kV were carried out.

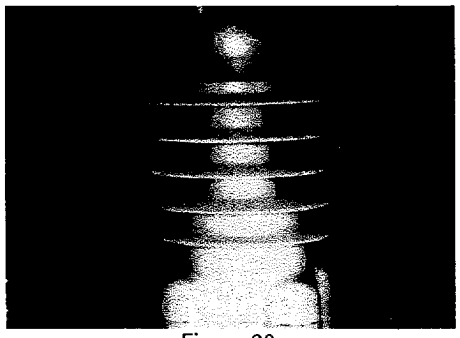

Figure 39.
Photograph of the 23 kV epoxy resin insulator.

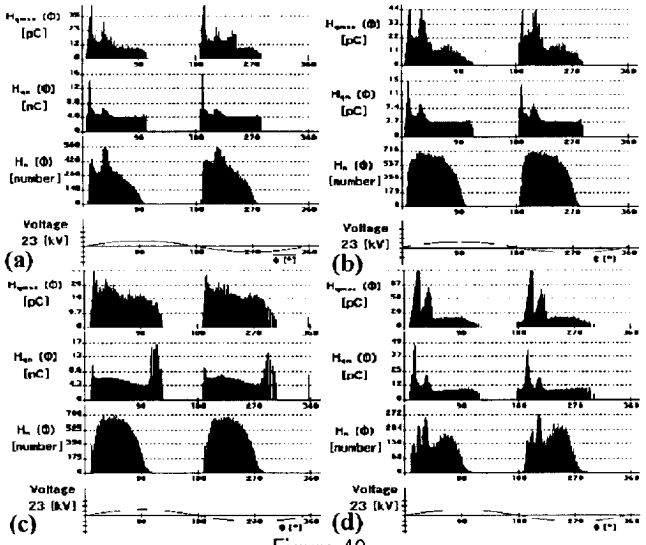

Figure 40.

Typical phase-resolved distributions as observed until breakdown during 0 to 1606 h aging of 23 kV epoxy resin insulator. (a) Aging 117 h, (b) 309 h, (c) 794 h, (d) 1415 h.

The clustering of the measured data was analyzed in a similar way as in the previous Section. From the beginning of the test until breakdown, six clusters of data were distinguished. To describe each of these clusters a data bank was developed representing consecutive aging stages of the insulator. In Figure 40 four typical phase-resolved distributions are shown, and in Table 1 the corresponding classification results are presented.

In Figure 41 this time behavior of the cluster formation of measured data is compared to the behavior of the maximum discharge magnitude as a function of the aging time. In this way additional information has been created which can be important in the judgement of the insulation quality [54].

This example shows the possibility of a digital PD analyzer for recognition of significant changes in dielectrics

Table 1.
Classification using data bank 'clustering: 23 kV insulator' as processed for the measuring data in Figure 40.

Stage	117 h	309 h	794 h	1415 h
1	100%			
2		91%		
3			100%	
4				
5				78%
6				

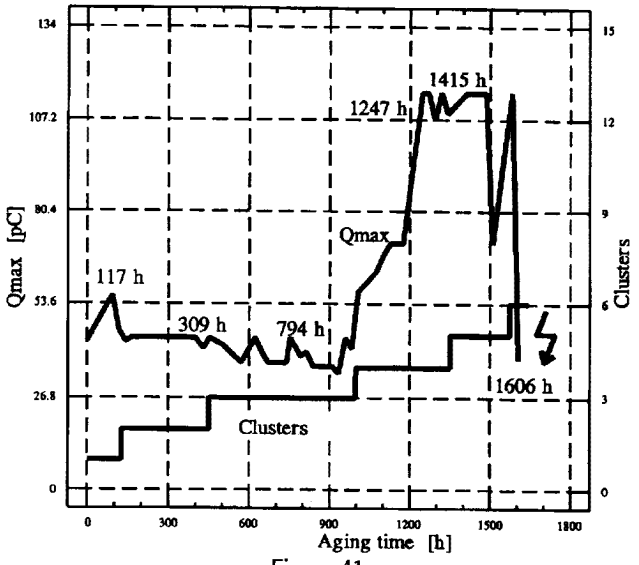

Figure 41.
Maximum discharge magnitude measured for 23 kV epoxy resin insulator during 1606 h aging until breakdown extended by clustering of phase-resolved distributions.

as observed during aging.

5. CONCLUSIONS AND SUGGESTIONS

IN this paper some actual aspects of digital analysis of PD have been discussed and the following conclusions are drawn.

The use of digital processing of PD requires additional calibration and performance verification. With regard to the discharge phase and magnitude, as well as the repetition rate, digital PD analysis offers much improvement for evaluating classic PD measurements.

It has been shown, that in practical cases a digital PD system provides additional information, can support the documentation and analysis of the PD measurement, can help to inventory and evaluate different measurements, but is not able to replace 100% of our working experience.

The discussion of this paper and others in the present Issue could lay the foundation for a more systematic analysis of the different digital techniques and statistical tools, which are used in the field of recognition and diagnosis of discharges in HV components. To analyze the whole range of modern PD evaluation techniques, the following further studies are suggested.

It is necessary to compare quantities which are useful for the evaluation of results obtained with phase-resolved (classical) PD detection and with time-resolved (UHF) detection.

The recognition techniques should be compared for type of discharges and the degradation stages of the insulation using UHF and classical detection.

Finally, an analysis is needed of the applicability of results as obtained from physical models of discharges for the evaluation of full scale HV apparatus.

REFERENCES

[1] A. E. W. Austen, S. Whitehead, "Discharges in Insulation under Alternating Current Stresses", Journal IEE, Vol. 88, Part II, pp. 18–22, 1941.

[2] E. C. Rogers, "The Self Extinction of Gaseous Discharges in Cavities in Dielectrics", Proc. IEE, Vol. 105, part A, pp. 621–630, 1958.

[3] F. H. Kreuger, *Detection and Location of Discharges in Particular in Plastic-insulated HV Cables*, Thesis Delft University 1960, P. 16–30.

[4] D. Koenig, *Erfassung von Teilentladungen in Hoehlraeumen von Epoxydharzplatten Zur Beurteilung Des Alterungsverhalten Bei Wechselspannung*, pp. 4–8, Thesis TH Braunschweig 1967.

[5] E. Neudert, R. Porzel, "Ein Oszillografisches Verfahren Zum Beurteilen von Teilentladungen", Elektrie, Vol. 9, pp. 360–362, 1968.

[6] *Partial Discharge Measurements*, IEC Publication 270, 1968, 1981.

[7] CIGRE, "Recognition of Discharges", Electra, Vol. 11, Dec. 1969.

[8] R. A. Bartnikas, "Simple Pulse-height Analyzer for PD Measurements", IEEE Trans. Instrumentation and Measurement, Vol. 18, no 4, pp. 341–345, Dec. 1969.

[9] F. H. Kreuger, *Partial Discharge Detection in HV Equipment*, 1969, Heywood, London, 1989, Butterworths, London.

[10] G. Mole, "Measurement of the Magnitude of Internal Corona in Cables", IEEE Trans. Power Apparatus and Systems, Vol. 89, pp. 776–780, 1970.

[11] H. G. Kranz, "Rechnerische Untersuchung Des Ein- Und Aussetzverhaltens von TE Bei Wechselspannung", ETZ-A, Vol. 94, H. 3, pp. 175–177, 1973.

[12] R. Bartnikas, "Corona Pulse Probability Density Function Measurements on Primary Distribution Power Cables", IEEE Trans. on Power Apparatus and Systems, Vol. 94, No. 3, pp. 716–723, May/june 1975.

[13] J. Austin, R. E. James, "On-line Digital Computer System for Measurement of Partial Discharges in Insulation Structures", IEEE Trans. EI, Vol. 11, pp. 129–139, 1976.

[14] J. Beinert, E. A. Kadry, W. Schuppe, "Die Bedeutung Der Teilentladungsmessung Fuer Die Erkenning von Stoerstellen Bei Kunststoffisolierten Mittelspannungskabeln", Elektrizitaetswirtschaft, Vol. 76, H. 26, pp. 925–928, 1977.

[15] K. G. Burnley, J. L. T. Exon, "Relationship between Various Measurement Techniques for Void Discharges", IEE Proc. Vol. 129 Part A, no. 8, pp. 593–6–6, Nov. 1982.

[16] S. A. Boggs, G. C. Stone, "Fundamental Limitation in the Measurement of Corona and PD", IEEE Trans. Electrical Insulation, Vol. 17 No. 2, pp. 143–150, April 1982.

[17] F. Rochon, T. Malewski, G. Vallancourt, " Acquisition and Processing of PD Measurement during Power Transformer Testing", pp. 546–554, Conf. on Dielec. Phenomena, Claymont, USA, 1984.

[18] R. Haller, E. Gulski, "Automatisierte Erfassung Und Verarbeitung von TE-signalen", Elektrie, Vol. 38, H. 10, pp. 383–385, 1984.

[19] G. Vallancourt, R. Malewski, D. Train, " Comparison of three Techniques of PD Measurement in Power Transformers", IEEE Trans. Power Apparatus and System, Vol. 104, No. 4, pp. 900–909, April 1985.

[20] R. Schifani, "A Novel Histogram for PD Signals in HV Insulation Systems", IEEE Trans. EI, Vol. 21, pp. 89–99, 1986.

[21] T. Okamoto, T. Tanaka, "Prediction of Treeing Breakdown from Pulse Height of Partial Discharges in Voltage-phase Angle", J. Jap, Vol. 24, No. 2, pp. 156–16, February 1985.

[22] T. Okamoto, T. Tanaka, "Novel PD-measurement Computer Aided Measurement System", IEEE Trans. Electrical Insulation, Vol. 21, No. 6, pp. 1015–1019, December 1986.

[23] R. Bartnikas, "A Commentary on PD Measurement and Detection", IEEE Trans. Electrical Insulation, Vol. 22, No 5, pp. 629–653, Oct. 1987.

[24] J. D. Gassaway, P. B. Jacob, C. A. Vassiliadis, "Computer-aided PD Measurement and Recognition", Paper 41.03, Fifth. Int. Symp. on HV Braunschweig 1987,

[25] R. E. Wotton, "Computer Assistance for the Performance Test and Interpretation of HV-ac Discharge", Paper 41.12, Fifth Int. Symp. on HV Braunschweig, 1987.

[26] F. H. Kreuger, E. Gulski, "Simultane Erfassung Und Verarbeitung von Teilentladungskenngroessen Zur Beurteilung Elektrischer Isolierungen", Technisches Messen, Vol. 55, H. 1, pp. 17–22, 1988.

[27] R. E. James, S. L. Jones, "Some Aspects of the Statistical Modeling of PD Inception Condition", IEEE Trans Electrical Insulation, Vol. 23 No. 2, pp. 297–306, April 1988.

[28] E. Gulski, F. H. Kreuger, "Digital Computer Sytem for Measurements of PD in Insulation Structures", Proc. 3rd Conf. on Cond. and Breakd. in Solid Diel. Trondheim Juli 3–6, pp. 582–586. 1989.

[29] D. Kurrat, D. Peier, "Fundamental Principles and Design of Digital Partial Discharge Measurement System", Proc. 3rd Conf. on Cond. and Breakd. in Solid Diel. Trondheim Juli 3–6, pp. 244–248, 1989.

[30] F. H. Kreuger, E. Gulski, "Automatisiertes Messsystem Zur Erfassung von Teilentladungskenngroessen Fuer Beurteilung Elektrischer Isolierungen", Technisches Messen, Vol. 56, H. 3, pp. 124–129, 1989.

[31] R. Krump, *Ein Störresistentes Verfahren Zur Computergestützten TE-diagnostik in SF_6 Schaltanalgen*, Thesis of Wuppertal University, 1989

[32] A. Pedersen, "On the Electrodynamics of PD in Voids in Solid Dielectrics", Trondheim, Proc. 3rd Conf. on Cond. and Breakd. in Solid Diel. pp. 107–116, July 3–6, 1989.

[33] B. H. Ward, "Digital Techniques for PD Measurements", IEEE Panel Session, Digital Techniques in HV Tests, Long Beach, pp. 83–87. July 11 1989.

[34] B. Fruth, G. Liptak, T. Ulrich, L. Niemeyer, "Aging of Rotating Machines Insulation- Mechanisms, Measurement Techniques", Proc. 3rd Conf. on Cond. and Breakd. in Solid Diel. pp. 597–601, Juli 3–6, Trondheim 1989.

[35] E. Gulski, F. H. Kreuger, "Computer-aided Analysis of Discharge Patterns", J. Phys. D: Appl. Phys., Vol. 23, pp. 1569–157, 1990.

[36] E. Gulski, F. H. Kreuger, "Computer-aided Recognition of Discharge Sources", Proc of IEEE Inter. Workshop on PD Measurement and their Traceability, Como, 4–6 September 1990.

[37] S. A. Boggs, "Partial Discharge: Overview and Signal Generation", IEEE Electrical Insulation Magazine, Vol. 6, No. 4, pp. 33–42, July/august 1990.

[38] M. Hikita, K. Yamada, A. Nakamura, T. Mizutani, A. Oohasi, "Measurements of PD by Computer and Analysis of PD Distribution by the Monte Carlo Method", IEEE Trans. Electrical Insulation, Vol. 25, No. 3, pp. 453–468, June. 1990.

[39] J. Fuhr, M Haessig, B. Fruth, T. Kaiser, "PD-fingerprints of some HV Apparatus", Proc. of IEEE Int. Symp. on EI, pp. 129–132, Toronto, June 3–6, 1990.

[40] E. Gulski, P. H. F. Morshuis, F. H. Kreuger, "Automized Recognition of PD in Cavities", Japanese Journal of Applied Physics, Vol. 29, No. 7, pp. 1329–1335, July, 1990.

[41] E. Gulski, F. H. Kreuger, "Recognition of Discharge Sources using Statistical Tools", Proc. 3rd Inter. Conf. on Prop. and Appl. of Diel. Mat. Tokyo, July 8–12, Paper A-4, 1991.

[42] E. Gulski, F. H. Kreuger, "Computer-aided Recognition of Discharge Patterns", Proc. 7th Inter. Symp on HV Enging., Dresden, August 26–30, Paper 71.01, 1991.

[43] E. Gulski, *Computer-aided Recognition of PD Using Statistical Tools*, Delft University Press, 1991.

[44] G. C. Stone, "Practical Techniques for Measuring PD in Operating Equipment", Proc. of the 3rd Int. Conf. on Diel. Materials, Tokyo, pp. 12–17, July 8–12, 1991.

[45] J. Fuhr, B. Fruth, L. Niemeyer, D. Koenigstein, M. Haessing, F. Gutfleisch, "Generic Procedure for Classification of Aged Insulating Systems", Proc. of the 3rd Int. Conf. on Diel. Materials, pp. 35–38, Tokyo, July 8–12, 1991.

[46] E. Gulski, F. H. Kreuger, "Diagnosis of Insulation Systems Using Statistical Tools", Proc. of IEEE Int. Symp. on EI, pp. 393–397, Baltimore, June 7–10, 1992.

[47] Y. J. Kim, J. K. Nelson, "Assessment of Deterioration in Epoxy/mica Machine Insulation", IEEE Trans. on EI, Vol. 27, No 5, pp. 1026–1039, 1992.

[48] E. Gulski, "Computer-aided Measurement of PD in HV Equipment", IEEE Trans. on Elec. Insulation, Vol. 28, No. 6, pp. 969–983, 1993.

[49] Ch. Hantouche, D. Fortune, "Digital Measurement of PD in Full-sized Power Capacitors", IEEE Trans. on Elec. Insulation, Vol. 28, No. 6, pp. 1025–1032, 1993.

[50] E. Gulski, P. Seitz, "Computer-aided Registration and Analysis of PD in HV Equipment", Proceedings of 8th Inter. Symp. on HV Engineering, Yokohama Japan 1993.

[51] M. Cacciari, A. Contin, G. Rabach, G. C. Montanari, "Diagnosis of Practical Insulation Systems by PD Measurements in the Presence of Multi-discharge Phenomena", Proc. CEIDP, Pocono, USA, pp. 414–419, October 1993.

[52] F. H. Kreuger, E. Gulski, A. Krivda, "Classification of PD", IEEE Trans. on Elec. Insulation, Vol. 28, No. 6, pp. 917–931, 1993.

[53] T. R. Blackburn, R. E. James, B. T. Phung, S. L. Jones, "Advanced Techniques for Characterization of PD in Oil-impregnated and Gas Insulated Systems", Paper 15–102, CIGRE Session, Paris 1994.

[54] F. H. Kreuger, P. H. F Morshuis, E. Gulski, "Evaluation of Discharge Damage By Fast Transient Detection and Statistical Analysis", Paper 15–106, CIGRE Session, Paris 1994.

[55] E. Gulski, A. Krivda, "Influence of Aging on Classification of Partial Discharges in High Voltage Components", IEEE Trans. on Diel. and Elect. Ins., Vol. 2, pp. 676–684, 1995.

[56] E. Gulski, "Diagnosis of HV Componenets by Digital PD Analyzer", IEEE Trans. on Diel. and Elect. Ins., Vol. 2, pp. 630–640, 1995.

[57] A. Krivda, E. Gulski, "Influence of Aging on Classification of PD in Cavities", Japan J. Appl. Phys., Vol. 33, pp. 5942–594, 1994.

[58] A. Krivda, E. Gulski, "Influence of Aging on Classification of PD", Proceedings of 9th Inter. Symp. on HV Engineering, Graz Austria, 1995.

[59] W. Boening, "Luftgehalt Und Luftspaltverteilung Geschichteter Dielectrica", Archiv Fuer Elektrotechnik, Vol. 48, pp. 7–22, 1963.

[60] A. Audoli, J. L. Drommi, "Generator and Motor Stator Monitoring Based on Partial Discharge Quadratic Rate Measurement", Proceedings of 1992 IEEE, Inter. Symp. on Electrical Insulation, pp. 359–36, Baltimore, 1992.

Manuscript was received on 20 April 1995.